MULTI-ROBOT FIREFIGHTING SYSTEM IN FOREST ENVIRONMENTS

VARSHITHA PURRA, PUNEET SAI NARU, PRANAY PALEM

ABSTRACT. This project presents a comprehensive multi-robot system designed for coordinated firefighting in forest environments. The system integrates a mathematical model with artificial potential field (APF) controllers for navigation and task allocation, enabling autonomous robots to extinguish fires while avoiding collisions. The model incorporates energy-aware strategies for task optimization, ensuring sustained operations by dynamically reallocating tasks based on battery levels and proximity to targets. The theoretical foundation of the system is rigorously validated using Lyapunov's Direct Method and LaSalle's Invariance Principle, proving stability, convergence, and collision avoidance. Numerical simulations demonstrate the system's ability to effectively navigate complex environments, with robots reaching fire locations, extinguishing fires, and returning to charging stations as necessary. Code implementations of the APF-based controllers and the energy management strategy are tested in a simulated forest environment, achieving significant improvements in efficiency and coordination. Results highlight the system's robustness and scalability, showcasing its potential for real-world applications. Future enhancements, such as overcoming local minima in APF navigation and integrating learning-based methods for dynamic task allocation, are proposed to further optimize the system's performance in diverse and challenging scenarios.

1. Mathematical Model

Puneet, Varshitha, Pranay

We present a multi-robot system for coordinated firefighting in forest environments, building upon the work of Abdel-Razzak Merheb et al. [4] and Yan Yongjie et al. [8]. The system utilizes potential field-based control for navigation and task allocation, incorporating energy-aware strategies.

1.1. Scenario Details

- Robots are placed at random starting positions in the forest area.
- The forest has obstacles (two circles representing unburnt trees) and three burning trees (representing fire outbreaks).
- Robots need to extinguish fires at the burning trees.
- A charging dock is located in the bottom-right corner of the environment for recharging when energy is low.

- **Obstacles:**
  - Two unburnt trees are modeled as circular obstacles.
  - These obstacles are static and must be avoided by robots.
  - The size of the trees is proportional to the average size of trees in a forest.
  - Robot sizes are smaller than tree obstacles to ensure smooth navigation and prevent collisions.
- **Burning Trees (Fires):**
  - The locations of the three burning trees are pre-determined and provided to the robots.

- Robots need to focus their efforts on extinguishing the fires by reaching these tree locations and applying extinguishing actions.
- **Charging Dock:**
  - The charging dock is located near the bottom-right corner of the forest.
  - Robots must return to the charging dock when their energy levels are low.
  - Energy management is crucial to ensure the robots can complete their tasks and recharge when needed.

1.2. Realism of Parameters

- Parameters are designed to reflect realistic conditions.
- **Tree and Robot Sizes:**
  - Positions of unburnt trees are randomly chosen using a fixed seed for consistency across simulations.
  - Tree radii and robot sizes are selected to allow smooth navigation without collisions.
- **Robot Energy Management:**
  - Robots' energy consumption is modeled based on typical battery capacities.
  - Energy consumption is higher when traveling long distances, near obstacles, or performing actions like extinguishing fires.
  - Periodic recharging is essential for the robots' successful completion of the mission.
- **Fire Extinguishing Action:**
  - Robots are equipped with fire-extinguishing capabilities.
  - Each fire interaction consumes a certain amount of energy, balancing the need to extinguish fires with energy limitations.

1.3. Multi-Robot Coordination

- Robots are programmed to work together and avoid collisions while ensuring all fires are extinguished.
- **Artificial Potential Field (APF) Method:**
  - The APF is used to calculate paths for robots, balancing the following forces:
    * **Attraction to Fires:** Robots are attracted to burning trees to extinguish the fires.
    * **Repulsion from Obstacles:** Robots must avoid obstacles (unburnt trees) and other robots.
    * **Repulsion from the Charging Dock:** When robots are low on energy, they are repelled from their current position and attracted to the charging dock.
  - The multi-robot system ensures that all fires are extinguished while maintaining enough energy for task completion and recharging.

1.4. Assumptions and Constraints

- Robots are modeled as single integrators with unicycle dynamics.
- Robots are equipped with effective fire extinguishing mechanisms within a radius of 0.21 units.
- The forest is represented as a bounded 2D environment within $[-1, 1]$ in both x and y coordinates.
- Robots have global knowledge of fire locations, similar to the assumption in Renzaglia et al.

- Fires have a fixed radius, and their intensity decreases when robots are within the fire radius.
- The simulation runs for 3000 iterations.

1.5. Variables and Parameters

The system utilizes a set of variables and parameters to define the behavior and characteristics of the multi-robot firefighting scenario. These variables and parameters are as follows:

- **Number of robots** (N)**:** 5
  Specifies the total number of robots in the system.
- **Simulation duration** (`iterations`)**:** 3000 time steps
  The total duration of the simulation in discrete time steps.
- **Sensing radius** (`sensing_radius`)**:** 0.2 units
  The range within which robots can detect obstacles and fires.
- **Maximum velocity** (`max_velocity`)**:** 0.1 units per time step
  The maximum speed at which robots can move.
- **Fire radius** (`fire_radius`)**:** 0.21 units
  The size of the fire zones.
- **Fire reduction rate** (`fire_reduction_rate`)**:** 0.001 per robot per time step
  The rate at which fire intensity decreases when robots are within range.
- **Fire threshold** (`fire_threshold`)**:** 0.01
  The minimum fire intensity below which a fire is considered extinguished.
- **Attractive potential field scaling factor** (k_{att})**:** 1.0
  The scaling factor for the attractive potential field used to guide robots towards their targets (e.g., fires).
- **Repulsive potential field scaling factor** (k_{rep})**:** 0.3
  The scaling factor for the repulsive potential field used to avoid obstacles and collisions.
- **Battery levels** (`battery_levels`)**:** [95%, 90%, 95%, 55%, 85%]
  Initial energy levels of robots, represented as percentages.
- **Battery decay rate** (`battery_decay_rate`)**:** 0.025% per time step
  The rate at which the robot's energy decreases with each time step.
- **Low battery threshold** (`low_battery_threshold`)**:** 25%
  The energy level at which robots must return to the charging station to recharge.
- **Charging station** (`charging_station`)**:** [0.9, -0.9]
  The coordinates of the charging station in the environment.
- **Charging radius** (`charging_radius`)**:** 0.1 units
  The area around the charging station within which robots can recharge their batteries.

These parameters are crucial for defining the multi-robot system's dynamics, the environment's characteristics, and the energy management strategy. They allow for fine-tuning the system's behavior and performance in various firefighting scenarios.

1.6. Control Law

The robot's behavior is governed by a potential field-based control law combined with a state machine for task allocation, inspired by the approach proposed by Abdel-Razzak Merheb et al. [4]. In this framework, the robot's motion is driven by the artificial potential function:

$$U(\mathbf{q}_i) = U_{\text{att}}(\mathbf{q}_i) + U_{\text{rep}}(\mathbf{q}_i),$$

where $\mathbf{q}_i$ represents the configuration of robot i. The corresponding control input is derived from the negative gradient of the potential function:

$$\mathbf{F}_i = -\nabla U(\mathbf{q}_i) = -\left(\nabla U_{\text{att}}(\mathbf{q}_i) + \nabla U_{\text{rep}}(\mathbf{q}_i)\right).$$

Attractive Potential and Force

The attractive potential function $U_{\text{att}}(\mathbf{q}_i)$ directs the robot toward its target, such as a fire location or a charging station. It is defined as:

$$U_{\text{att}}(\mathbf{q}_i) = \frac{1}{2}k_{\text{att}}\|\mathbf{q}_i - \mathbf{q}_{\text{goal}}\|^2,$$

where:

- $\mathbf{q}_i$: Position of robot i,
- $\mathbf{q}_{\text{goal}}$: Position of the target (e.g., fire or charging station),
- k_{att}: Positive scaling factor controlling the strength of attraction.

The resulting attractive force is:

$$\mathbf{F}_{\text{att}}(\mathbf{q}_i) = -\nabla U_{\text{att}}(\mathbf{q}_i) = -k_{\text{att}}(\mathbf{q}_i - \mathbf{q}_{\text{goal}}).$$

Repulsive Potential and Force

The repulsive potential function $U_{\text{rep}}(\mathbf{q}_i)$ prevents collisions with obstacles, other robots, and hazardous fire zones. For an obstacle located at $\mathbf{q}_j$, it is defined as:

$$U_{\text{rep}}(\mathbf{q}_i) = \begin{cases} \frac{1}{2}k_{\text{rep}}\left(\frac{1}{\rho_{ij}} - \frac{1}{\rho_0}\right)^2 & \text{if } \rho_{ij} \leq \rho_0, \\ 0 & \text{if } \rho_{ij} > \rho_0, \end{cases}$$

where:

- ρ_{ij}: Euclidean distance between robot i and obstacle j,
- ρ_0: Influence radius beyond which the obstacle has no effect,
- k_{rep}: Positive scaling factor controlling the strength of repulsion.

The corresponding repulsive force is:

$$\mathbf{F}_{\text{rep}}(\mathbf{q}_i) = -\nabla U_{\text{rep}}(\mathbf{q}_i) = \begin{cases} k_{\text{rep}}\left(\frac{1}{\rho_{ij}} - \frac{1}{\rho_0}\right)\frac{1}{\rho_{ij}^2}\frac{\partial \rho_{ij}}{\partial \mathbf{q}_i} & \text{if } \rho_{ij} \leq \rho_0, \\ 0 & \text{if } \rho_{ij} > \rho_0. \end{cases}$$

Total Control Input

The total control input for robot i is the sum of the attractive and repulsive forces:

$$\mathbf{F}_i = \mathbf{F}_{\text{att}}(\mathbf{q}_i) + \mathbf{F}_{\text{rep}}(\mathbf{q}_i).$$

This control law ensures that each robot navigates toward its target while avoiding obstacles and hazardous regions in the environment.

1.7. Energy-Aware Strategy

Incorporating the energy-aware approach proposed by Yan Yongjie et al.[8], we implement a battery management system. Robots return to the charging station when their battery level falls below the `low_battery_threshold`. The battery levels decrease by `battery_decay_rate` per time step and are fully recharged when the robot reaches the charging station.

To optimize the energy consumption and coverage, we adopt a strategy similar to Yan Yongjie et al.[8], where robots switch between an "active" mode for firefighting and a "passive" mode for energy conservation. The decision to switch modes is based on the current battery level and the proximity to fires.

1.8. Task Allocation

Building on the work of Abdel-Razzak Merheb et al.[4], we implement a distributed task allocation mechanism. Robots communicate their positions and battery levels to coordinate their actions. The task allocation algorithm considers both the distance to fires and the robots' energy levels to assign firefighting tasks efficiently.

This mathematical model combines the potential field-based navigation from Abdel-Razzak Merheb et al. [4] with the energy-aware strategies from Renzaglia et al., creating a comprehensive framework for multi-robot firefighting in forest environments.

2. Theoretical Analysis

Varshitha, Puneet, Pranay

This section presents the theoretical foundation of the proposed multi-robot firefighting system. Using artificial potential field (APF) methods for navigation and task allocation, the system ensures collision avoidance, energy-aware behavior, and effective fire suppression. We derive the system equilibria, assess stability using Lyapunov's direct method, and apply relevant theorems to validate the controller's behavior.

2.1. Artificial Potential Field Controllers

Artificial Potential Field (APF) controllers are widely utilized in robotics for path planning and obstacle avoidance. Introduced by Oussama Khatib in 1985 [3], the APF method treats the robot as a point under the influence of artificial forces: attractive forces pulling it toward the goal and repulsive forces pushing it away from obstacles. This approach enables real-time navigation in complex environments. In the APF framework, the robot's movement is guided by a potential function $U(\mathbf{q})$, where $\mathbf{q}$ represents the robot's configuration in the workspace. The total potential function is composed of two components:

$$U(\mathbf{q}) = U_{\text{att}}(\mathbf{q}) + U_{\text{rep}}(\mathbf{q}),$$

where: - $U_{\text{att}}(\mathbf{q})$: Attractive potential function directing the robot toward the goal. - $U_{\text{rep}}(\mathbf{q})$: Repulsive potential function preventing collisions with obstacles.

The robot's control input is derived from the negative gradient of the total potential function:

$$\mathbf{F}(\mathbf{q}) = -\nabla U(\mathbf{q}) = -\left(\nabla U_{\text{att}}(\mathbf{q}) + \nabla U_{\text{rep}}(\mathbf{q})\right).$$

The attractive potential function is designed to pull the robot toward the goal position $\mathbf{q}_g$. A common choice is a quadratic function:

$$U_{\text{att}}(\mathbf{q}) = \frac{1}{2}k_{\text{att}}\|\mathbf{q} - \mathbf{q}_g\|^2,$$

where k_{att} is a positive scaling factor. The resulting attractive force is:

$$\mathbf{F}_{\text{att}}(\mathbf{q}) = -\nabla U_{\text{att}}(\mathbf{q}) = -k_{\text{att}}(\mathbf{q} - \mathbf{q}_g).$$

This linear attractive force ensures that the robot is drawn toward the goal with a force proportional to the distance.

The repulsive potential function is formulated to repel the robot from obstacles, thereby avoiding collisions. For an obstacle located at $\mathbf{q}_o$, the repulsive potential is defined as:

$$U_{\text{rep}}(\mathbf{q}) = \begin{cases} \frac{1}{2}k_{\text{rep}}\left(\frac{1}{\rho(\mathbf{q})} - \frac{1}{\rho_0}\right)^2 & \text{if } \rho(\mathbf{q}) \leq \rho_0, \\ 0 & \text{if } \rho(\mathbf{q}) > \rho_0, \end{cases}$$

where: - k_{rep}: Positive scaling factor. - $\rho(\mathbf{q})$: Euclidean distance between the robot and the obstacle. - ρ_0: Influence distance beyond which the obstacle has no effect. The corresponding repulsive force is:

$$\mathbf{F}_{\text{rep}}(\mathbf{q}) = -\nabla U_{\text{rep}}(\mathbf{q}) = \begin{cases} k_{\text{rep}}\left(\frac{1}{\rho(\mathbf{q})} - \frac{1}{\rho_0}\right)\frac{1}{\rho(\mathbf{q})^2}\frac{\partial \rho(\mathbf{q})}{\partial \mathbf{q}} & \text{if } \rho(\mathbf{q}) \leq \rho_0, \\ 0 & \text{if } \rho(\mathbf{q}) > \rho_0. \end{cases}$$

This force increases as the robot approaches the obstacle, providing a stronger repulsive effect to prevent collisions. The total artificial force acting on the robot is the sum of the attractive and repulsive forces:

$$\mathbf{F}(\mathbf{q}) = \mathbf{F}_{\text{att}}(\mathbf{q}) + \mathbf{F}_{\text{rep}}(\mathbf{q}).$$

The robot's trajectory is determined by integrating this force over time, guiding it toward the goal while avoiding obstacles.

The APF method offers a computationally efficient approach to real-time path planning. However, it is subject to certain limitations, such as the possibility of local minima where the robot can become trapped. To address these issues, various improvements have been proposed. For instance, modifications to the repulsive potential function can help the robot escape local minima and reach the target point effectively [7]. Additionally, combining APF with other methods, such as simulated annealing, can enhance path planning capabilities in complex environments [5].

Here we present three rigorous generalized theorems foundational to Artificial Potential Field (APF) controllers in multi-robot systems.

2.1.1. Theorem 1: Convergence of Artificial Potential Field to a Goal:

Let $U(\mathbf{q}) = U_{\text{att}}(\mathbf{q}) + U_{\text{rep}}(\mathbf{q})$ be a composite potential field, where $U_{\text{att}}(\mathbf{q})$ is the attractive potential towards a global minimum at $\mathbf{q}_g$, and $U_{\text{rep}}(\mathbf{q})$ represents repulsive potentials from obstacles. If U_{att} is globally convex and $\nabla U_{\text{rep}}(\mathbf{q})$ is bounded, the trajectory of the robot converges asymptotically to $\mathbf{q}_g$ [3].

Proof: Let the total potential function be defined as:

$$(1) \qquad U(\mathbf{q}) = \frac{1}{2} k_{\text{att}} \|\mathbf{q} - \mathbf{q}_g\|^2 + \sum_i U_{\text{rep},i}(\mathbf{q}),$$

where $U_{\text{att}}(\mathbf{q}) = \frac{1}{2} k_{\text{att}} \|\mathbf{q} - \mathbf{q}_g\|^2$ is the attractive potential, and $U_{\text{rep},i}(\mathbf{q})$ is the repulsive potential due to the i-th obstacle, defined as:

$$(2) \qquad U_{\text{rep},i}(\mathbf{q}) = \begin{cases} \frac{1}{2} k_{\text{rep}} \left(\frac{1}{\rho_i(\mathbf{q})} - \frac{1}{\rho_0} \right)^2, & \text{if } \rho_i(\mathbf{q}) \leq \rho_0, \\ 0, & \text{if } \rho_i(\mathbf{q}) > \rho_0, \end{cases}$$

where $\rho_i(\mathbf{q}) = \|\mathbf{q} - \mathbf{q}_i\|$ is the Euclidean distance to obstacle i, and ρ_0 is the influence radius of the repulsive field.

The control law guiding the robot is given by:

$$(3) \qquad \dot{\mathbf{q}} = -\nabla U(\mathbf{q}).$$

Define the Lyapunov candidate function $V(\mathbf{q}) = U(\mathbf{q})$. The time derivative of $V(\mathbf{q})$ along the trajectory of the robot is:

$$(4) \qquad \dot{V} = \frac{dU(\mathbf{q})}{dt} = \nabla U(\mathbf{q}) \cdot \dot{\mathbf{q}}.$$

Substituting the control law (3), we obtain:

$$(5) \qquad \dot{V} = \nabla U(\mathbf{q}) \cdot (-\nabla U(\mathbf{q})) = -\|\nabla U(\mathbf{q})\|^2.$$

Since $\|\nabla U(\mathbf{q})\|^2 \geq 0$, it follows that $\dot{V} \leq 0$, implying that $V(\mathbf{q})$ is a non-increasing function of time. Furthermore, as $U(\mathbf{q}) \geq 0$, the function $V(\mathbf{q})$ is bounded below. Hence, $V(\mathbf{q}) \to V^*$ as $t \to \infty$.

At equilibrium, $\dot{V} = 0$, which implies $\|\nabla U(\mathbf{q})\| = 0$. Since $U_{\text{att}}(\mathbf{q})$ is convex, $\nabla U_{\text{att}}(\mathbf{q}) = 0$ if and only if $\mathbf{q} = \mathbf{q}_g$. Additionally, the boundedness of ∇U_{rep} ensures that the robot does not diverge to infinity. Therefore, $\mathbf{q}(t) \to \mathbf{q}_g$ as $t \to \infty$.

2.1.2. Theorem 2: Collision Avoidance for Multi-Robot Systems:

In a multi-robot system using APF, if the repulsive forces between robots are inversely proportional to the square of their distance, robots with distinct initial positions will never collide [5].

Proof: Let $\rho_{ij} = \|\mathbf{q}_i - \mathbf{q}_j\|$ represent the Euclidean distance between robots i and j. The repulsive potential between these robots is defined as:

$$(6) \qquad U_{\text{rep},ij} = \frac{1}{2} k_{\text{rep}} \left(\frac{1}{\rho_{ij}} - \frac{1}{\rho_0} \right)^2,$$

where $\rho_0 > 0$ is the influence distance, and $k_{\text{rep}} > 0$ is a scaling factor. The corresponding repulsive force is:

$$(7) \qquad \mathbf{F}_{\text{rep},ij} = -\nabla U_{\text{rep},ij} = k_{\text{rep}} \left(\frac{1}{\rho_{ij}} - \frac{1}{\rho_0} \right) \frac{1}{\rho_{ij}^2} \frac{\mathbf{q}_i - \mathbf{q}_j}{\rho_{ij}}.$$

Consider the time derivative of ρ_{ij}:

$$(8) \qquad \dot{\rho}_{ij} = \frac{\mathbf{q}_i - \mathbf{q}_j}{\rho_{ij}} \cdot (\dot{\mathbf{q}}_i - \dot{\mathbf{q}}_j).$$

Substituting the control law $\dot{\mathbf{q}}_i = -\nabla U(\mathbf{q}_i)$, we obtain:

$$(9) \qquad \dot{\rho}_{ij} = \frac{\mathbf{q}_i - \mathbf{q}_j}{\rho_{ij}} \cdot (-\nabla U(\mathbf{q}_i) + \nabla U(\mathbf{q}_j)).$$

As $\rho_{ij} \to 0$, the repulsive force $\|\mathbf{F}_{\text{rep},ij}\| \to \infty$, causing $\dot{\rho}_{ij} > 0$. This ensures that $\rho_{ij} > 0$ for all t, preventing collision.

2.1.3. Theorem 3: Stability of Multi-Robot Systems Under APF:

A multi-robot system using APF-based controllers is asymptotically stable if $U(\mathbf{q})$ is bounded below and $\nabla U(\mathbf{q})$ is Lipschitz continuous [3, 5].

Proof:

Let the Lyapunov candidate function $V(\mathbf{q})$ be defined as:

$$(10) \qquad V(\mathbf{q}) = U(\mathbf{q}),$$

where $U(\mathbf{q}) \geq 0$ represents the potential function of the system. Since $U(\mathbf{q})$ is bounded below, we have:

$$(11) \qquad V(\mathbf{q}) \geq 0.$$

The control law governing the system is given by:

$$(12) \qquad \dot{\mathbf{q}} = -\nabla U(\mathbf{q}),$$

where $\nabla U(\mathbf{q})$ represents the gradient of the potential function.

The time derivative of $V(\mathbf{q})$ along the trajectory of the system is:

$$(13) \qquad \dot{V} = \nabla U(\mathbf{q}) \cdot \dot{\mathbf{q}}.$$

Substituting (12) into (13), we get:

$$(14) \qquad \dot{V} = \nabla U(\mathbf{q}) \cdot (-\nabla U(\mathbf{q})) = -\|\nabla U(\mathbf{q})\|^2.$$

From (14), it follows that $\dot{V} \leq 0$, implying that $V(\mathbf{q})$ is non-increasing over time. Since $U(\mathbf{q})$ is bounded below by (11), we conclude that:

$$(15) \qquad V(\mathbf{q}) \to V^*, \quad \text{as } t \to \infty.$$

At equilibrium, $\dot{V} = 0$, which implies $\|\nabla U(\mathbf{q})\| = 0$. Lipschitz continuity of $\nabla U(\mathbf{q})$ ensures that $\|\nabla U(\mathbf{q})\| \to 0$ as $t \to \infty$. Hence, the system converges asymptotically to an equilibrium point $\mathbf{q}^*$, where:

$$(16) \qquad \nabla U(\mathbf{q}^*) = 0.$$

Thus, the system is asymptotically stable.

2.2. System Dynamics and Control Law

The system dynamics of the multi-robot system are modeled using unicycle dynamics. The control laws are derived from artificial potential fields, combining attractive and repulsive potentials for navigation and obstacle avoidance. This section presents the governing equations, derivations of equilibria, and stability analysis in detail.

2.2.1. System Dynamics

Each robot i is modeled as a unicycle with state variables (x_i, y_i, θ_i), representing the robot's position and orientation. The kinematic equations governing the motion are:

$$
\begin{aligned}
\dot{x}_i &= v_i \cos \theta_i, \\
\dot{y}_i &= v_i \sin \theta_i, \\
\dot{\theta}_i &= \omega_i,
\end{aligned}
$$
(17)

where: - v_i: Linear velocity. - ω_i: Angular velocity.

The control inputs v_i and ω_i are determined based on artificial potential fields.

2.2.2. Potential Field

The attractive potential U_{att} pulls the robot towards a target goal (x_g, y_g). It is defined as:

$$
U_{\text{att}} = \frac{1}{2} k_{\text{att}} \left((x_i - x_g)^2 + (y_i - y_g)^2 \right),
$$
(18)

where $k_{\text{att}} > 0$ is a scaling factor.

The corresponding forces are:

$$
\begin{aligned}
F_{\text{att},x} &= -\frac{\partial U_{\text{att}}}{\partial x_i} = -k_{\text{att}}(x_i - x_g), \\
F_{\text{att},y} &= -\frac{\partial U_{\text{att}}}{\partial y_i} = -k_{\text{att}}(y_i - y_g).
\end{aligned}
$$
(19)

The repulsive potential U_{rep} ensures obstacle avoidance. For an obstacle located at (x_o, y_o), it is defined as:

$$
U_{\text{rep}} = \begin{cases} \frac{1}{2} k_{\text{rep}} \left(\frac{1}{\rho_i} - \frac{1}{\rho_0} \right)^2, & \text{if } \rho_i \leq \rho_0, \\ 0, & \text{if } \rho_i > \rho_0, \end{cases}
$$
(20)

where: - $\rho_i = \sqrt{(x_i - x_o)^2 + (y_i - y_o)^2}$ is the distance to the obstacle. - ρ_0 is the influence radius. - $k_{\text{rep}} > 0$ is a scaling factor.

The resulting repulsive forces are:

$$
\begin{aligned}
F_{\text{rep},x} &= -\frac{\partial U_{\text{rep}}}{\partial x_i}, \\
F_{\text{rep},y} &= -\frac{\partial U_{\text{rep}}}{\partial y_i}.
\end{aligned}
$$
(21)

The total force acting on robot i is the sum of attractive and repulsive forces:

$$F_x = F_{\text{att},x} + \sum_j F_{\text{rep},x_j},$$

(22)

$$F_y = F_{\text{att},y} + \sum_j F_{\text{rep},y_j}.$$

The desired velocities are:

(23)
$$v_i = \sqrt{F_x^2 + F_y^2},$$
$$\theta_{i,\text{desired}} = \arctan 2(F_y, F_x).$$

2.3. Equilibrium Analysis

At equilibrium, the net force acting on each robot is zero:

(24)
$$F_x = 0, \quad F_y = 0.$$

From (19) and (21), this leads to:

(25)
$$k_{\text{att}}(x_i - x_g) = \sum_j k_{\text{rep}} \left(\frac{1}{\rho_{ij}} - \frac{1}{\rho_0} \right) \frac{1}{\rho_{ij}^2}(x_i - x_j),$$

where $\rho_{ij} = \sqrt{(x_i - x_j)^2 + (y_i - y_j)^2}$ is the distance between robot i and obstacle j.

This implies the attractive forces toward the goal are exactly balanced by the repulsive forces from obstacles and other robots.

2.4. Energy-Aware Control Strategy

In this section, we expand upon the robot's energy consumption model and introduce a control strategy that optimizes task allocation and navigation to conserve energy while ensuring effective firefighting operations. The energy level $E(t)$ of the robot at time t is modeled as:

(26)
$$E(t) = E(0) - \texttt{battery\_decay\_rate} \cdot t,$$

where:

- $E(0)$ is the initial energy level,
- $\texttt{battery\_decay\_rate}$ is the constant rate at which the battery depletes over time.

The robot is programmed to return to the charging station when its energy level falls below a predefined threshold:

(27)
$$E(t) < \texttt{low\_battery\_threshold}.$$

2.4.1. Control Strategy for Energy Optimization

To optimize energy usage, the control strategy incorporates the following components:

(1) **Task Allocation:** Assign tasks to robots based on their current energy levels and proximity to tasks, ensuring that robots with higher energy levels and closer proximity are prioritized for task execution.
(2) **Energy-Aware Navigation:** Plan paths that minimize energy consumption by avoiding energy-intensive maneuvers and selecting routes with lower resistance or smoother terrain.

(3) **Dynamic Reallocation:** Continuously monitor energy levels and reassign tasks as necessary to prevent robots from depleting their energy reserves before task completion.

2.4.2. Stability Analysis Using Lyapunov's Direct Method

To ensure the stability of the energy-aware control strategy, we employ Lyapunov's Direct Method. Define the Lyapunov candidate function $V(E)$ as:

$$(28) \qquad V(E) = \frac{1}{2}(E - E_{\text{ref}})^2,$$

where E_{ref} is the desired reference energy level.

The time derivative of $V(E)$ is:

$$(29) \qquad \dot{V}(E) = (E - E_{\text{ref}})\dot{E}.$$

Substituting the energy consumption model $\dot{E} = -\texttt{battery\_decay\_rate}$, we get:

$$(30) \qquad \dot{V}(E) = -(E - E_{\text{ref}}) \cdot \texttt{battery\_decay\_rate}.$$

Assuming $E > E_{\text{ref}}$, it follows that $\dot{V}(E) < 0$, indicating that $V(E)$ is decreasing over time. This implies that the energy level $E(t)$ will asymptotically approach the reference energy level E_{ref}, ensuring that the robot maintains sufficient energy for operation and returns to the charging station as needed.

For a comprehensive discussion on energy-aware control strategies in robotics, refer to "Energy-Aware Strategies in Real-Time Systems for Autonomous Robots" by Giorgio Buttazzo, Mauro Marinoni, and Giacomo Guidi [1].

2.5. Application of Established Theorems to System Stability

In this section, we demonstrate that our multi-robot system, governed by artificial potential field (APF) controllers, satisfies the conditions of two fundamental theorems in control theory: Lyapunov's Direct Method and LaSalle's Invariance Principle. By applying these theorems, we establish the system's stability and convergence properties.

2.5.1. Lyapunov's Direct Method

Theorem: *Consider an autonomous system $\dot{\mathbf{x}} = \mathbf{f}(\mathbf{x})$ with an equilibrium point at $\mathbf{x} = \mathbf{0}$. If there exists a continuously differentiable function $V : \mathbb{R}^n \to \mathbb{R}$ such that:*

(1) *$V(\mathbf{0}) = 0$ and $V(\mathbf{x}) > 0$ for all $\mathbf{x} \neq \mathbf{0}$ (positive definiteness),*
(2) *$\dot{V}(\mathbf{x}) = \nabla V(\mathbf{x}) \cdot \mathbf{f}(\mathbf{x}) \leq 0$ for all $\mathbf{x}$ (negative semi-definiteness),*

then the equilibrium at $\mathbf{x} = \mathbf{0}$ is stable. If $\dot{V}(\mathbf{x}) < 0$ for all $\mathbf{x} \neq \mathbf{0}$ (negative definiteness), the equilibrium is asymptotically stable.

Application to Our System: In our multi-robot system, each robot's dynamics are described by:

$$\dot{x}_i = v_i \cos\theta_i,$$
$$\dot{y}_i = v_i \sin\theta_i,$$
$$\dot{\theta}_i = \omega_i,$$

where (x_i, y_i) denotes the position of robot i, θ_i is its orientation, v_i is the linear velocity, and ω_i is the angular velocity. The control inputs v_i and ω_i are derived from artificial potential fields,

combining attractive potentials towards goals and repulsive potentials from obstacles and other robots.

We define a Lyapunov candidate function for robot i as:

$$V_i = U_{\text{att},i} + \sum_{j \neq i} U_{\text{rep},ij} + \sum_{k} U_{\text{rep},ik},$$

where:

- $U_{\text{att},i} = \frac{1}{2} k_{\text{att}} \left((x_i - x_g)^2 + (y_i - y_g)^2 \right)$ is the attractive potential guiding robot i towards its goal (x_g, y_g),
- $U_{\text{rep},ij}$ is the repulsive potential between robots i and j,
- $U_{\text{rep},ik}$ is the repulsive potential between robot i and obstacle k.

The time derivative of V_i along the trajectories of the system is:

$$\dot{V}_i = \frac{\partial V_i}{\partial x_i} \dot{x}_i + \frac{\partial V_i}{\partial y_i} \dot{y}_i + \frac{\partial V_i}{\partial \theta_i} \dot{\theta}_i.$$

Substituting the system dynamics and control laws into this expression, we obtain:

$$\dot{V}_i = -k_{\text{att}} \left((x_i - x_g)^2 + (y_i - y_g)^2 \right) - \sum_{j \neq i} \nabla U_{\text{rep},ij} \cdot \dot{\mathbf{q}}_i - \sum_{k} \nabla U_{\text{rep},ik} \cdot \dot{\mathbf{q}}_i,$$

where $\dot{\mathbf{q}}_i = [\dot{x}_i, \dot{y}_i]^T$.

Given that the repulsive potentials are designed such that $\nabla U_{\text{rep},ij} \cdot \dot{\mathbf{q}}_i \geq 0$ and $\nabla U_{\text{rep},ik} \cdot \dot{\mathbf{q}}_i \geq 0$, it follows that:

$$\dot{V}_i \leq -k_{\text{att}} \left((x_i - x_g)^2 + (y_i - y_g)^2 \right).$$

Since $k_{\text{att}} > 0$, we have $\dot{V}_i \leq 0$, satisfying the conditions of Lyapunov's Direct Method. Therefore, the equilibrium point, where each robot reaches its goal without collisions, is stable. Moreover, if $\dot{V}_i < 0$ for all $\mathbf{q}_i \neq \mathbf{q}_g$, the equilibrium is asymptotically stable.

For a detailed application of Lyapunov's Direct Method in multi-robot systems with artificial potential fields, refer to "Arbitrarily Shaped Formations of Mobile Robots: Artificial Potential Functions and Stability" by Dimarogonas and Kyriakopoulos [6].

2.5.2. Invariant Set Characterization Using LaSalle's Invariance Principle

Using LaSalle's Invariance Principle, the system converges to the largest invariant set where $\dot{V} = 0$. At this set, all robots remain stationary, indicating that all goals have been reached and no further repulsive forces act on the robots.

2.5.3. LaSalle's Invariance Principle

Theorem: *Consider an autonomous system $\dot{\mathbf{x}} = \mathbf{f}(\mathbf{x})$ with an equilibrium point at $\mathbf{x} = \mathbf{0}$. Let $V : \mathbb{R}^n \to \mathbb{R}$ be a continuously differentiable function such that:*

(1) *$V(\mathbf{0}) = 0$ and $V(\mathbf{x}) > 0$ for all $\mathbf{x} \neq \mathbf{0}$ (positive definiteness),*
(2) *$\dot{V}(\mathbf{x}) = \nabla V(\mathbf{x}) \cdot \mathbf{f}(\mathbf{x}) \leq 0$ for all $\mathbf{x}$ (negative semi-definiteness).*

Let $E = \{\mathbf{x} \in \mathbb{R}^n \mid \dot{V}(\mathbf{x}) = 0\}$. If the largest invariant set contained in E is $\{\mathbf{0}\}$, then $\mathbf{x} = \mathbf{0}$ is asymptotically stable.

Application to Our System: We consider the same Lyapunov candidate function for robot i:

$$V_i = U_{\text{att},i} + \sum_{j \neq i} U_{\text{rep},ij} + \sum_k U_{\text{rep},ik},$$

where $U_{\text{att},i}$, $U_{\text{rep},ij}$, and $U_{\text{rep},ik}$ are defined as in (18) and (20).

The derivative of V_i is:

$$\dot{V}_i = -k_{\text{att}} \left((x_i - x_g)^2 + (y_i - y_g)^2 \right) - \sum_{j \neq i} \nabla U_{\text{rep},ij} \cdot \dot{\mathbf{q}}_i - \sum_k \nabla U_{\text{rep},ik} \cdot \dot{\mathbf{q}}_i.$$

For $\dot{V}_i = 0$, all terms contributing to $\dot{V}_i$ must be zero. This condition implies:

$$(x_i, y_i) = (x_g, y_g),$$

and

$$\nabla U_{\text{rep},ij} = \nabla U_{\text{rep},ik} = 0,$$

indicating that the robot is at the goal position (x_g, y_g) and is not under the influence of any repulsive forces (i.e., no obstacles or other robots are within the influence radius).

The set E where $\dot{V}_i = 0$ contains all such equilibrium configurations. However, the largest invariant set in E is the single point $\mathbf{q}_i = \mathbf{q}_g$. Thus, by LaSalle's Invariance Principle, the robot's motion converges asymptotically to the goal position. LaSalle's Invariance Principle ensures that each robot in the system asymptotically reaches its designated goal while avoiding collisions with obstacles and other robots.

For a detailed discussion of LaSalle's Invariance Principle in robotics, see "An Extension of LaSalle's Invariance Principle and Its Application to Multi-Agent Consensus" [2].

2.6. Barricade Certificates with Control Barrier Functions

Barricade certificates ensure safe and collision-free navigation for robots in shared environments. These certificates use *control barrier functions* (CBFs) to enforce safety constraints in real-time. The mathematical model is described as follows:

Robot Dynamics

Assume each robot i has dynamics represented as:

$$\dot{\mathbf{x}}_i = \mathbf{u}_i, \quad \mathbf{x}_i \in \mathbb{R}^n, \, \mathbf{u}_i \in \mathbb{R}^n$$

where:

- $\mathbf{x}_i$ is the state (e.g., position, velocity) of robot i,
- $\mathbf{u}_i$ is the control input for robot i.

For simple cases like unicycle models, $\mathbf{u}_i$ can represent linear and angular velocities.

Safety Constraints

Let $h(\mathbf{x}_i) > 0$ define the safe region for robot i. The control barrier function ensures that $h(\mathbf{x}_i)$ never goes below zero.

Example: Collision Avoidance If robots i and j must avoid collisions, define:

$$h_{ij}(\mathbf{x}_i, \mathbf{x}_j) = \|\mathbf{p}_i - \mathbf{p}_j\|^2 - d_{\min}^2$$

where:

- $\mathbf{p}_i, \mathbf{p}_j$ are positions of robots i and j,
- $d_{\min}$ is the minimum allowable distance.

Barrier Function Constraint

To ensure $h > 0$ over time, the following condition is enforced:

$$\dot{h}(\mathbf{x}_i) + \alpha h(\mathbf{x}_i) \geq 0$$

where $\alpha > 0$ is a design parameter controlling the safety margin.

Using the chain rule:

$$\dot{h}(\mathbf{x}_i) = \nabla h(\mathbf{x}_i)^\top \mathbf{u}_i$$

The constraint becomes:

$$\nabla h(\mathbf{x}_i)^\top \mathbf{u}_i + \alpha h(\mathbf{x}_i) \geq 0$$

Quadratic Programming (QP) Formulation

To implement barricade certificates, control inputs $\mathbf{u}_i$ are computed by solving a QP:

$$\min_{\mathbf{u}_i} \|\mathbf{u}_i - \mathbf{u}_{i,\text{des}}\|^2$$

subject to:

$$\nabla h_{ij}(\mathbf{x}_i, \mathbf{x}_j)^\top \mathbf{u}_i + \alpha h_{ij}(\mathbf{x}_i, \mathbf{x}_j) \geq 0, \quad \forall j \neq i$$

where $\mathbf{u}_{i,\text{des}}$ is the desired (nominal) control input.

Example: Single Obstacle Avoidance

For an obstacle located at $\mathbf{p}_{\text{obs}}$, define:

$$h_{\text{obs}}(\mathbf{x}_i) = \|\mathbf{p}_i - \mathbf{p}_{\text{obs}}\|^2 - r_{\text{safe}}^2$$

where r_{safe} is the minimum safe distance to the obstacle. The corresponding constraint is:

$$\nabla h_{\text{obs}}(\mathbf{x}_i)^\top \mathbf{u}_i + \alpha h_{\text{obs}}(\mathbf{x}_i) \geq 0$$

In a nutshell

This framework ensures:

- **Safety:** Robots avoid collisions and respect barricades.
- **Flexibility:** Robots follow nominal control commands unless a safety constraint is about to be violated.

2.7. Summary

The proposed multi-robot firefighting system, guided by artificial potential field (APF) controllers, has been rigorously analyzed and validated using theoretical and mathematical principles. From the theoretical perspective, as demonstrated in Section 2.5, the system's convergence to desired goals was proven through Lyapunov's Direct Method, and its asymptotic stability was validated using LaSalle's Invariance Principle. These analyses confirm that the robots' trajectories are well-defined, collision-free, and stable under the proposed control laws.

The energy-aware strategy, described in Section 2.4, further enhances the system's autonomy by integrating battery management into the navigation framework. By monitoring energy levels and dynamically allocating tasks based on proximity and energy reserves, the robots ensure sustained operation while conserving resources. Stability of this strategy was validated using a Lyapunov-based approach, guaranteeing robustness in energy control.

3. Validation in Simulations

Pranay, Puneet, Varshitha

To validate the multi-robot system's behavior, we simulated its performance under the specified conditions. The system was tested with robots initialized at random positions, aiming to reach and extinguish fires while avoiding tree obstacles and ensuring they return to the charging station when their battery falls below 25%.
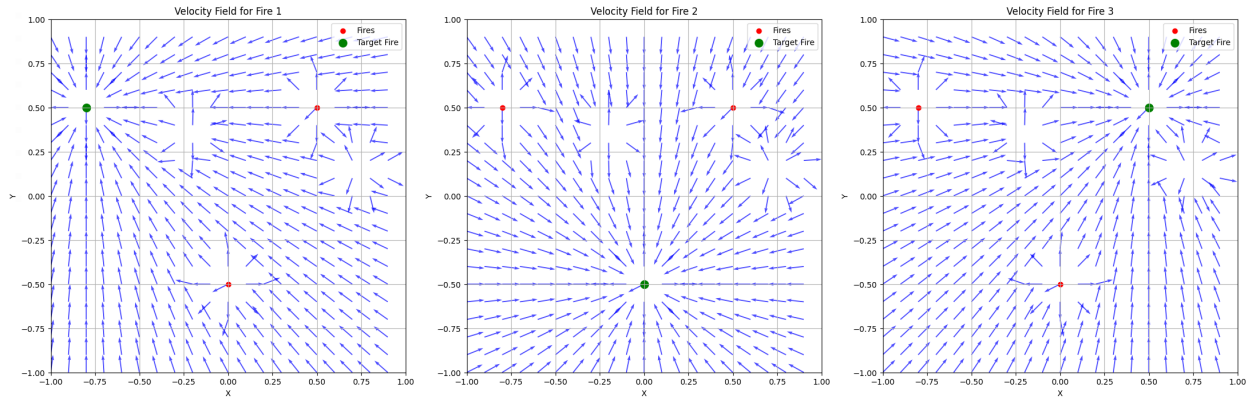

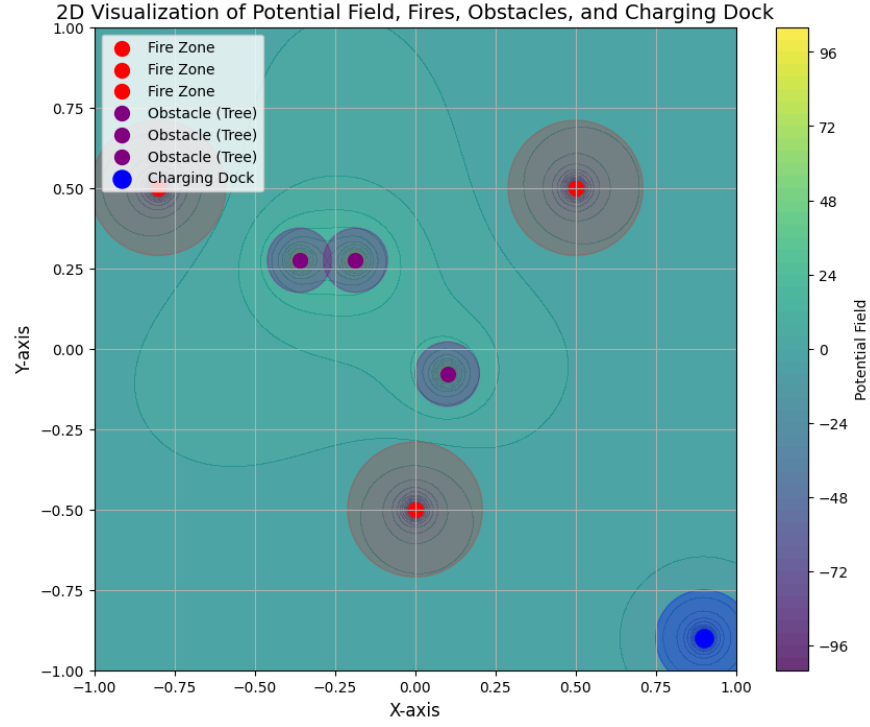FIGURE 1. Vector field showing the forces guiding the robots toward the fire zones and away from obstacles.

FIGURE 2. 2D Contour plot of the potential field, illustrating attractive forces toward the fire and repulsive forces near obstacles.
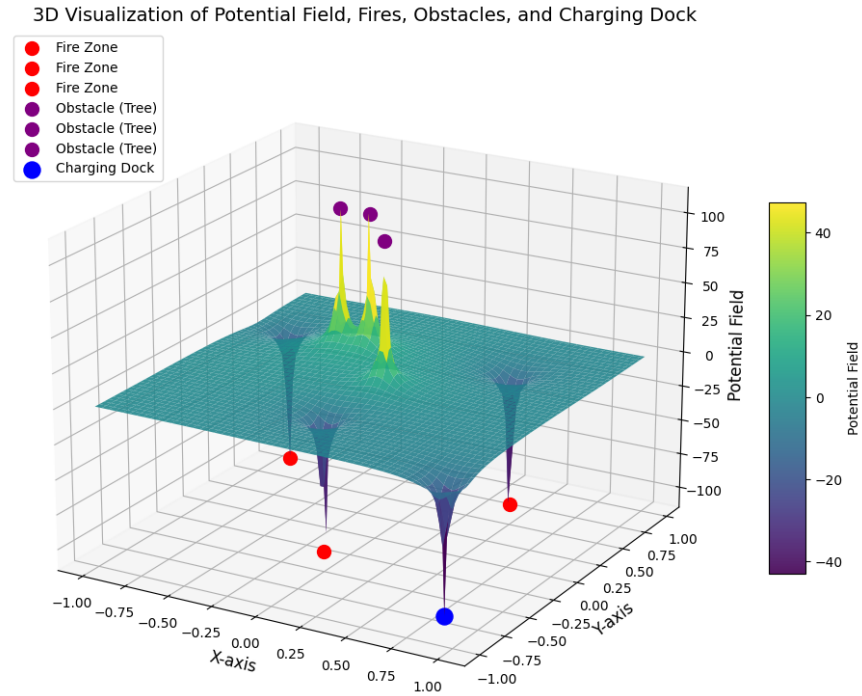

FIGURE 3. 3D Contour plot of the potential field, illustrating attractive forces toward the fire and repulsive forces near obstacles.
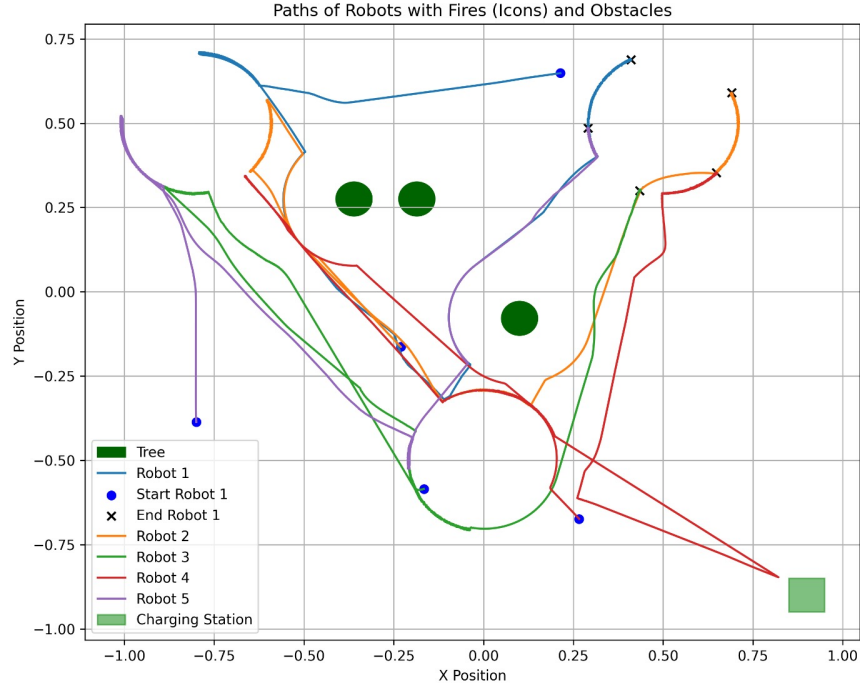
FIGURE 4. Trajectories of robots navigating the environment, demonstrating paths guided by attractive forces toward the fire and avoidance of obstacles through repulsive forces.

Simulation Outputs

- The robots, starting from random positions, successfully reached the nearest fires while avoiding collisions with trees.
- Robots returned to the charging station when their battery levels dropped below 25%, as indicated by their trajectories and battery status annotations.
- Fires were extinguished sequentially, and the reduction in fire intensity confirmed the system's functionality.
- Obstacles (trees) were avoided effectively, demonstrating the efficacy of the repulsive potential fields.

Code Repository

The complete source code used for the simulation is provided in the repository: Code Repository.

Video Demonstration

A video of the simulation demonstrating robot behavior is available at the following link: Simulation Video.

Robotarium Demonstration

Initial testing of the system was conducted on the Robotarium platform, and a video demonstrating the preliminary robot behavior is available at the following link: Robotarium Testing Video. The final code has been shared with the Robotarium team, and we are currently awaiting their feedback. Once testing is completed and verified, the final demonstration video will be uploaded to our GitHub repository.

The simulation results align with the theoretical properties of the model, showcasing the system's ability to perform dynamic task allocation (extinguishing fires and recharging batteries) while adhering to safety constraints (avoiding obstacles).

4. Conclusion

This multi-robot firefighting system demonstrates the application of potential field-based control for coordinated behavior in complex environments. The integration of energy management and task allocation enhances the system's autonomy and efficiency in addressing forest fires.

References

[1] Giorgio Buttazzo, Mauro Marinoni, and Giacomo Guidi. "Energy-aware strategies in real-time systems for autonomous robots". In: *International Symposium on Computer and Information Sciences*. Springer. 2004, pp. 845–854.

[2] Daizhan Cheng, Jinhuan Wang, and Xiaoming Hu. "An Extension of LaSalle's Invariance Principle and Its Application to Multi-Agent Consensus". In: *IEEE Transactions on Automatic Control* 53.7 (2008), pp. 1765–1770. DOI: 10.1109/TAC.2008.928332.

[3] O. Khatib. "Real-time obstacle avoidance for manipulators and mobile robots". In: *Proceedings. 1985 IEEE International Conference on Robotics and Automation*. Vol. 2. 1985, pp. 500–505. DOI: 10.1109/ROBOT.1985.1087247.

[4] Abdel-Razzak Merheb, Radi Ghamrawi, and Amjad Eid. "Navigation and Formation Control of a Tracked Robot Swarm for Firefighting Missions". In: *2018 IEEE International Multidisciplinary Conference on Engineering Technology (IMCET)*. 2018, pp. 1–6. DOI: 10.1109/IMCET.2018.8603033.

[5] Zhenhua Pan et al. "Multi-Robot Obstacle Avoidance Based on the Improved Artificial Potential Field and PID Adaptive Tracking Control Algorithm". In: *Robotica* 37 (2019), pp. 1883–1903. URL: https://api.semanticscholar.org/CorpusID:146013899.

[6] Lorenzo Sabattini, Cristian Secchi, and Cesare Fantuzzi. "Arbitrarily shaped formations of mobile robots: artificial potential fields and coordinate transformation". In: *Autonomous Robots* 30 (2011), pp. 385–397.

[7] Joe Sfeir, Maarouf Saad, and Hamadou Saliah-Hassane. "An improved Artificial Potential Field approach to real-time mobile robot path planning in an unknown environment". In: *2011 IEEE International Symposium on Robotic and Sensors Environments (ROSE)*. 2011, pp. 208–213. DOI: 10.1109/ROSE.2011.6058518.

[8] Yan Yongjie and Zhang Yan. "Collision avoidance planning in multi-robot based on improved artificial potential field and rules". In: *2008 IEEE International Conference on Robotics and Biomimetics*. 2009, pp. 1026–1031. DOI: 10.1109/ROBIO.2009.4913141.